Available at www.sciencedirect.com

ScienceDirect

journal homepage: www.elsevier.com/locate/watres

Modeling microbial diversity in anaerobic digestion through an extended ADM1 model

Ivan Ramirez[a,b], Eveline I.P. Volcke[a,c], Rajagopal Rajinikanth[a,d], Jean-Philippe Steyer[a,*]

[a]INRA, UR50, Laboratoire de Biotechnologie de l'Environnement, Avenue des Etangs, Narbonne F-11100, France
[b]Department of Automation, University of Ibague, Tolima, Colombia
[c]Department of Applied Mathematics, Biometrics and Process Control, Ghent University, Coupure links 653, 9000 Gent, Belgium
[d]Department of Civil Engineering, Indian Institute of Technology, Roorkee 247667, Uttarakhand, India

ARTICLE INFO

Article history:
Received 10 November 2008
Received in revised form
15 March 2009
Accepted 22 March 2009
Published online 1 April 2009

Keywords:
ADM1
Anaerobic digestion
Microbial diversity
Diversity index
Organic shock load
Pulse disturbance
UASFB

ABSTRACT

The anaerobic digestion process comprises a whole network of sequential and parallel reactions, of both biochemical and physicochemical nature. Mathematical models, aiming at understanding and optimization of the anaerobic digestion process, describe these reactions in a structured way, the IWA Anaerobic Digestion Model No. 1 (ADM1) being the most well established example. While these models distinguish between different micro-organisms involved in different reactions, to our knowledge they all neglect species diversity between organisms with the same function, i.e. performing the same reaction. Nevertheless, available experimental evidence suggests that the structure and properties of a microbial community may be influenced by process operation and on their turn also determine the reactor functioning. In order to adequately describe these phenomena, mathematical models need to consider the underlying microbial diversity. This is demonstrated in this contribution by extending the ADM1 to describe microbial diversity between organisms of the same functional group. The resulting model has been compared with the traditional ADM1 in describing experimental data of a pilot-scale hybrid Upflow Anaerobic Sludge Filter Bed (UASFB) reactor, as well as in a more detailed simulation study. The presented model is further shown useful in assessing the relationship between reactor performance and microbial community structure in mesophilic CSTRs seeded with slaughterhouse wastewater when facing increasing levels of ammonia.

1. Introduction

The anaerobic digestion process for wastewater treatment can nowadays be considered as state-of-the art technology. Because of its sustainable characteristics, i.e. high capacity to treat slowly degradable substrates at high concentrations, low energy requirements, reduction of odors and the possibility for energy recovery and reduced CO_2 emissions compared to other techniques, it is yet widely applied and its application is expected to further increase in future. Anaerobic digestion is a multi-step process in which organic carbon is converted into biogas, being a mixture of mainly carbon dioxide (CO_2) and methane (CH_4). Besides physicochemical reactions, the process comprises two types of biochemical reactions: extracellular (disintegration and hydrolysis) and intracellular ones. The latter type involves a variety of

* *Corresponding author*. Tel.: +33 468 425 163; fax: +33 468 425 160.
E-mail address: steyer@supagro.inra.fr (J.-P. Steyer).
0043-1354/$ – see front matter © 2009 Elsevier Ltd. All rights reserved.
doi:10.1016/j.watres.2009.03.034

microorganisms, namely fermentative bacteria (i.e. acidogens, responsible for the uptake of sugar and amino acids), hydrogen-producing and acetate-forming bacteria (i.e. acetogens, degrading long chain fatty acids, valerate, butyrate and propionate), and archaea which convert acetate or hydrogen into methane (i.e. methanogens). Other types of anaerobes play important roles in establishing a stable environment at various stages of methane fermentation. An example of the latter are homoacetogens, which can oxidize or synthesize acetate depending on the external hydrogen concentration (Kotsyurbenko, 2005).

Despite their distinct advantages, the application of anaerobic digestion systems is often limited by the fact that they are sensitive to disturbances and may suffer from instability. Such instability is usually witnessed as a drop in the methane production rate, a drop in the pH and/or a rise in the volatile fatty acid (VFA) concentration, leading to digester failure. Such failure can be caused by various inhibitory substances, one of them being ammonia (Chen et al., 2008). High ammonia concentrations, originating from the degradation of organic proteineous material, are often encountered during anaerobic digestion of animal wastes such as slaughterhouse waste, swine manure, cattle and poultry wastes and industrial wastes originating from food processing. Although ammonia is an important buffer in the process, and it is an essential nutrient for anaerobic microbes, high ammonia concentrations can decrease microbial activities, particularly for methanogens (Angelidaki and Ahring, 1993), resulting in a disturbed balance between fermentation and methanogenesis, which may lead to a fatal upset of the anaerobic treatment process. Within two distinct methanogenic groups, acetate-consuming methanogens are usually found to be more sensitive to high ammonia concentrations than hydrogen-utilizing ones (Hansen et al., 1998; Sprott and Patel, 1986), although some studies also indicate hydrogen-utilizing methanogens as the most sensitive group (Wiegant and Zeeman, 1986).

Given that Free Ammonia Nitrogen (FAN) rather than Total Ammonia Nitrogen (TAN) is suggested as the actual toxic agent, an increase in pH will result in increased toxicity (Borja et al., 1996). Process instability due to ammonia often results in volatile fatty acids' (VFAs) accumulation, which again leads to a decrease in pH and thereby declining concentration of FAN. Most studies on inhibition of anaerobic digestion by ammonia reported in literature determine inhibition thresholds rather than the dynamic behavior of microorganisms upon toxicant addition and their adaptation to elevated ammonia concentrations. Nevertheless, an example of the species selection during process start-up is described by Calli et al. (2005). These authors detected, through 16S rDNA/rRNA based molecular methods, a shift in the population of acetoclastic methanogens, from *Methanosaeta* to *Methanosarcina*, during start-up of five up flow anaerobic reactors seeded with different sludges, under gradually increasing ammonia levels.

Mathematical models have proven their effectiveness in process design and operation. With respect to anaerobic digestion, the Anaerobic Digestion Model No. 1 (ADM1, Batstone et al., 2002), developed by the corresponding International Water Association (IWA) Task Group, has become widespread and generally accepted. However, ADM1 does not distinguish between microorganisms performing the same reaction – which implies all of them are assumed to have the same properties – and can therefore not adequately represent or predict experimental results concerning this type of interspecies diversity. The need for incorporation of detailed micro-scale data into current wastewater treatment models was also indicated previously by Yuan and Blackall (2002), regarding the influence of plant design and operation on microbial community structure and microbial properties in activated sludge systems.

This contribution presents an approach for modeling microbial diversity in the anaerobic digestion process, applied to the standard ADM1 which has been extended with multiple species for each reaction. The extended model has subsequently been applied to handle microbial diversity in both normal conditions, not leading to process imbalance, and abnormal situations, characterized by the presence of inhibiting ammonia levels in the reactor.

2. Materials and methods

2.1. Experimental setup

A laboratory scale Upflow Anaerobic Sludge Filter Bed (UASFB) reactor (diameter 12 cm; height 117 cm; effective volume 9.8 L) was used in this study. The reactor column was made up of Plexiglas and constituted of two compartments: the bottom part was operated as a UASB reactor whereas the top part was operated as an anaerobic filter. The top portion of the UASFB reactor was randomly packed with 90 pieces of small cylindrical, buoyant polyethylene packing media (height: 29 mm; diameter: 30–35 mm; density: 0.93 kg/m^3), and baffled with 16 partitions. Fifty percent of the reactor volume (excluding the headspace of 30 cm height) was filled with the packing media. The reactor, operated at $33 \pm 1\,^{\circ}C$, was equipped with a continuous internal recirculation system from top to the bottom (recirculation rate: 9 L/h). Recirculation was done mainly to eliminate the possibility of high organic loading close to the feed port and to favor better wastewater/sludge contact. The digester was seeded with granules (15% by total volume) originating from a UASB digester treating cheese wastewaters.

This hybrid UASFB reactor was operated for a total period of 232 days at $33 \pm 1\,^{\circ}C$. Continuous feeding of the reactor was started with an initial OLR of 3.1 gCOD/L d. OLR was then increased stepwise by increasing the substrate concentration from 3.1 to 21.7 g/L (around 95% of the total COD was soluble), while maintaining a constant HRT of 1.15 days. A COD_s removal efficiency of 80% was considered as the threshold level in the present study for the operation of the UASFB reactor. The OLR was progressively increased by 20–30% once or twice a week until the COD_s removal dropped below 80%. The feed was supplemented with nutrients to attain a COD:N:P ratio of 400:7:1 in the wastewater. The feed pH was adjusted to 6–6.5 using a 6 N sodium hydroxide. The performance of the UASFB reactor was monitored as described by Rajinikanth et al. (2008).

The experiments were performed with distillery vinasse (wine residue after distillation), which was obtained from a local distillery around Narbonne, France.

In this type of wastewater, soluble COD is mainly present as monosaccharides (S_{su} in ADM1) and little as amino acids (S_{aa}) and long chain fatty acids (S_{fa}). Particulate COD is mainly present in the form of carbohydrates (X_{ch}), besides some composites (X_c), proteins (X_{pr}) and lipids (X_{li}). The input VFA values were calculated from measured concentrations of acetate (S_{ac}), propionate (S_{pro}), butyrate (S_{bu}) and valerate (S_{va}). The initial pH resulted from the ionized forms of VFAs, bicarbonate, ammonia and cation/anion concentrations. Ammonia (S_{IN}) and bicarbonate (S_{IC}) were measured by Kelj-dahl's method and using a TOC meter, respectively. Anion concentration (S_{an}) was taken equal to S_{IN} and cation concentration (S_{cat}) was adjusted in each case according to the initial experimental pH. The concentrations of these individual components used in the model as process inputs can be found in Rajinikanth et al. (2008).

2.2. *Model structure*

The IWA Anaerobic Digestion Model No. 1 (ADM1, Batstone et al., 2002) was extended to handle microbial diversity within functional groups. In the traditional ADM1 model, one microbial population is associated to each reaction. Seven functional groups of microorganisms are distinguished, corresponding to the degradation of sugar (by X_{su}), amino acids (by X_{aa}), LCFA (by X_{fa}), valerate and butyrate (by X_{c4}), propionate (by X_{pro}), acetate (by X_{ac}) and hydrogen (by X_{h2}) and one microbial population is associated to each reaction. In order to account for microbial diversity, the traditional ADM1 model was extended in such a way that multiple species are associated to each functional group. The number of species per reaction is arbitrary and in this study has been set to 10, to keep a reasonable computation speed. This approach is detailed in Appendix A for the sugar degraders (X_{su}, state variable 17) involved in sugar degradation (reaction 5), and subject to decay (reaction 13). Its application to the remaining populations (state variables 18–23) with respect to the corresponding degradations (reactions 6–12) and decay reactions (reactions 14–19) is straightforward.

Whereas the original ADM1 possesses 24 state variables, of which 7 biomass species (7 functional groups, 1 species per functional group), the extended model includes 70 different biomass species (7 functional groups, 10 species per functional group), of 87 state variables in total. The number of associated reactions is extended from 19 to 154. The resulting model will further be denoted as ADM1_10, where '10' refers to the extension of the original model for microbial diversity with 10 species for each group. Within each functional group, species may differ in terms of their yield coefficient Y as well as Monod maximum specific uptake rate k_m and half saturation constant K_s. In this sense, species may be different not only in the sense handled by microbial taxonomists (e.g. using 97% sequence similarity in 16S rRNA genes), but also when belonging to the same genus.

In our case, the yield coefficient was assumed constant as in reality the variability of this parameter is low. Within a functional group, the kinetic parameters k_m and K_s were randomly chosen from a normal bimodal distribution, with means of $\mu_1 = 0.6 \times k$, $\mu_2 = 1.4 \times k$, and standard deviations of $\sigma_{1,2} = 0.125 \times k$ where k is the value of the corresponding standard ADM1 parameter. The distribution type and their parameter values were established following a curve-fitting process using experimental data from a UASFB reactor. This approach adds a stochastic component to ADM1_10, compared to the deterministic ADM1. It is clear that many other approaches to define the microbial properties within functional groups can be thought of. They are all likely to be stochastic since microbial properties cannot be defined with certainty. In order to maintain comparable conditions for simulations, the initial biomass concentrations in ADM1 will be distributed equally among the corresponding microbial populations in ADM1_10.

Biomass retention in the UASFB reactor has been modeled in the simplified way suggested in the ADM1 report (Batstone et al., 2002), with a term including the residence time of solids ($t_{res,x}$) in the biomass mass balance equation to account for the difference between hydraulic retention time (HRT) and solid retention time (SRT). The resulting model has been implemented in MATLAB™/Simulink. Its applicability has first been tested by Ramirez and Steyer (2008) to model anaerobic digestion in a fixed bed reactor. In this contribution, a thorough model validation has been performed on experimental data for UAFSB reactor. It is important to note that the presented modeling approach is generic and can also be applied to other processes. Volcke et al. (2008) demonstrated the applicability of a model including different species performing the same reaction, describing experimental nitrification data through a model with two types of ammonium oxidizers.

Developing and tuning mathematical models in normal situations are nowadays a well defined procedure that can be easily performed, even with complex models such as ADM1. However, developing and tuning a model to adequately represent abnormal situations is still a difficult and challenging task. In particular, when facing inhibition and/or toxicant, anaerobic digestion processes may experimentally present different behaviors that are still not fully understood: one process can indeed show high robustness with respect to the presence of a toxicant while another similar process is much more sensitive to this toxicant. It is indeed likely that different species will exhibit different behaviors towards these substances. The effect of non-reactive toxicant affecting all species has been examined by Ramirez and Steyer (2008). Other non-reactive toxicant such as ammonia inhibits a specific population, in this case methanogens.

In ADM1, all microbial mediated substrate conversion processes are subject to inhibition by extreme pH values. Moreover, anaerobic oxidation processes are subject to inhibition due to accumulation of hydrogen while acetoclastic methanogenesis is inhibited by high free ammonia concentrations. Inhibition caused by hydrogen and free ammonia was originally implemented in ADM1 by rate multipliers that reflect non-competitive inhibition and an empirical correlation was used to reflect the effects of extreme pH. All inhibitions from ADM1 were kept identical in the ADM1_10 model.

3. Results and discussion

The behavior of the modified anaerobic digestion model, ADM1_10, has been compared to the one of the standard ADM1 and to experimental results in simulating the behavior of a pilot-scale UASFB reactor operated under varying input OLR. Further comparison of the ADM1 and ADM1_10 has been performed for abnormal conditions, by simulating the effect of ammonia pulses. Finally, simulation results of ADM1_10 for a reactor exposed to increasing levels of ammonia were analyzed with respect to the relationship between reactor performance and microbial community structure. The results are described in what follows.

3.1. *Simulation of UASFB with varying OLR: ADM1 vs. ADM1_10*

Previous experience in simulating the behavior of a reactor fed with the same wine distillery wastewater (Ramirez and Steyer, 2008) led to the identification of the main ADM1 parameters which need to be modified in order to reasonably reflect the experimental data. Only the maximum specific substrate uptake rate (k_m) and the half saturation constant (K_s) for acetate and propionate were calibrated to fit the data. The resulting values were used in all simulations, with ADM1 as well as ADM1_10 (in the latter case as center values).

Fig. 1 compares the experimental data with the simulation results obtained with both models for the UASFB reactor operated at a varying input loading rate by varying the influent concentration while maintaining a constant HRT. As it is seen both models can simulate nicely the dynamic evolutions of the main variables, in the liquid and also in the gas phase. As a consequence, assessing the most appropriate model among ADM1 and ADM1_10 is a tedious, not to say impossible, task. Note that the main purpose of this study was not to perfectly fit these data but to evaluate the ability of both models to adequately predict the behavior of this particular digestion process. Soluble COD, VFAs and biogas production values are higher in ADM1 than in ADM1_10 since the amount of biomass from ADM1 is lower than the biomass from ADM1_10. This is in agreement with the diversity–productivity hypothesis of Tilman et al. (2002) and the phenomenon is known as "overyielding".

Between day 100 and 200, both models over-predicted VFA concentrations. It appeared that the simulated rate at which acetate was converted to methane under the load imposed was somewhat under-estimated. This may have resulted from either under-estimation of the substrate consumption coefficients for acetoclastic methanogenesis or an over-estimation of the inhibition of this activity by ammonia. The models predict well the dynamics of the biogas production rate and composition as a response of the load imposed. Small deviations in predicting the biogas production and quality have been found, which may be attributed to the fact that the standard ADM1 uses the same gas/liquid transfer coefficients for all gases (CO_2, CH_4, H_2), while this is not the case in reality. Besides, also the dependence of these coefficients on the specific reactor configuration applied has been neglected. The pH was also quite accurately simulated and the models were able to reflect the trends that were observed in experimental data. The pH prediction is closely related to the cation and anion concentrations in the reactor, and actually, the difference between the two concentrations. Since the ion

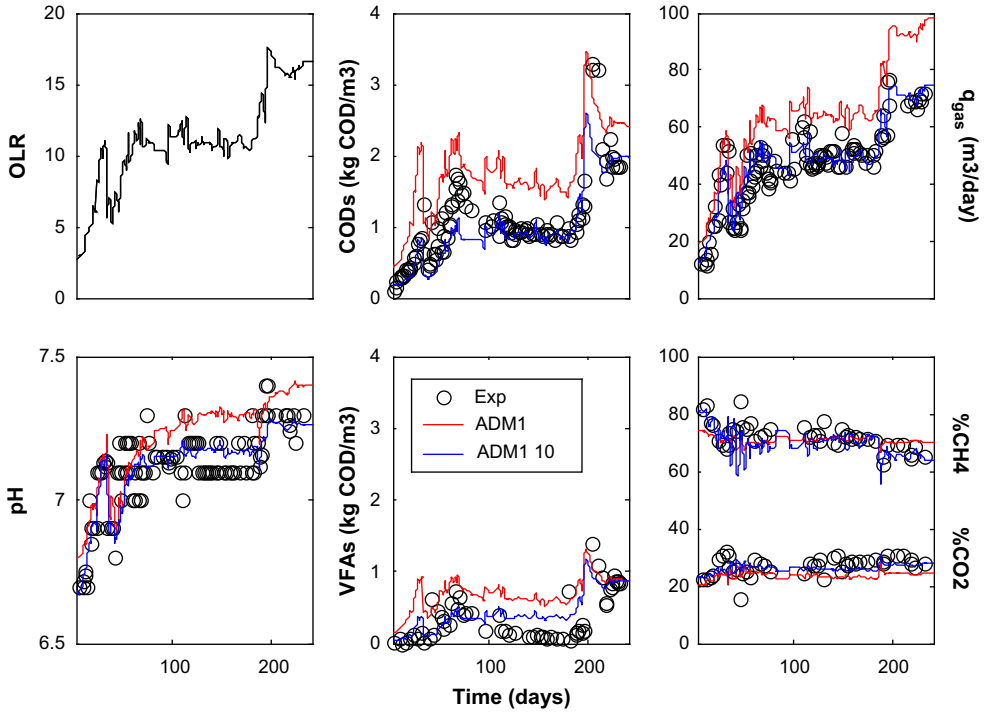

Fig. 1 – Behavior of a UAFSB reactor: experimental data versus simulation results with ADM1 and ADM1_10.

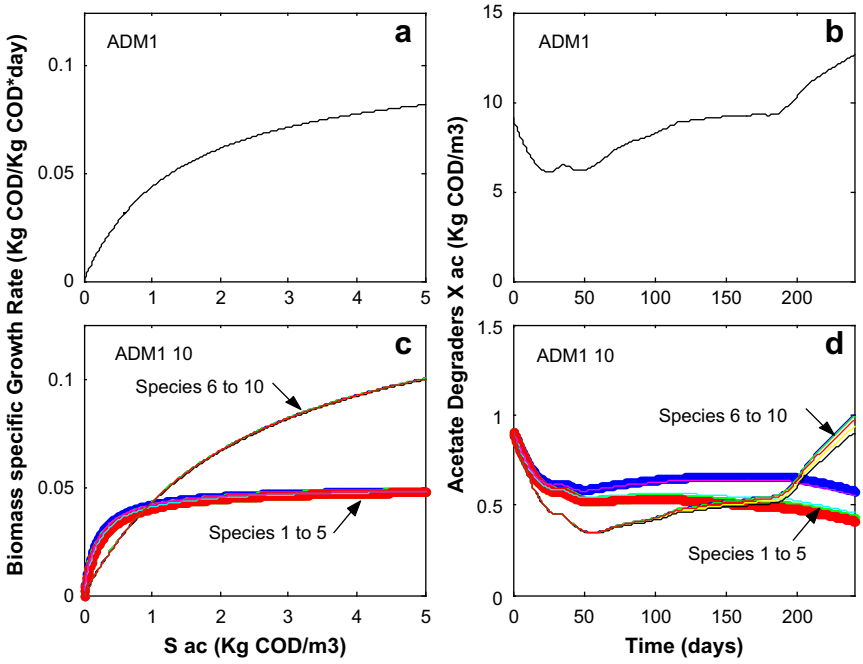

Fig. 2 – Specific growth rates (Monod curves) characterizing acetate degrading biomass in ADM1 (a) and ADM1_10 (c). Simulated evolution of acetate degrading biomass for ADM1 (b) and ADM1_10 (d) corresponding with macroscopic behavior of Fig. 1.

concentrations were not measured, it was then calculated using the pH value and taking into account the concentration of ammonia, alkalinity and VFA concentration in the reactor. The value of the input cation from the reactor minus the input anion concentration in the feed was arbitrarily increased in the models, so that the pH values were calibrated. On day 35, about 300 mL of sludge were accidentally discharged out of the reactor (connection failure at the bottom of the reactor) and hence the performance of the UASFB was disturbed. This disturbance was not included in the simulations and may be this explains the differences mainly in COD_s and VFAs between the simulated and experimental data during the period 35–57 days.

The main difference between the ADM1 and ADM1_10 models lies in the biomass evolutions. Fig. 2 shows the obtained specific growth rates and the dynamic evolution of acetate degraders during these simulations. Similar results were obtained for other degraders (not shown). The specific growth rate in terms of substrate concentrations (Monod curves) are depicted too. As it is seen in Fig. 2c we have two biomass groups: *K-strategists* (species 1–5) vs. *μ-strategists* (also known as *R-strategists*, species 6–10) which is related to the fact that we have combined high K_S values with high μ values and low K_S values with low μ values. After an initial decrease of all species, related to a decrease of total biomass, from day 150 on, species 6–10 outcompete species 1–5, (Fig. 2d), which is attributed to their higher growth rate (see Fig. 2c). At the same time, acetate concentration switches from low values to high ones (data not shown), leading to a competitive advantage of the biomass group of *μ-strategists*. This competitive advantage is also maintained for a longer simulation period: even after 3000 days, species 6–10 all survive (data not shown).

3.2. *ADM1 vs. ADM1_10 when facing a toxicant*

In this section, both models were applied to evaluate the performance of a digester facing a toxicant in the feeding line. To minimize simulation time, it was decided to simulate the behavior of a CSTR. Similar evolution of microbial populations would be obtained in a UASFB reactor but, due to biomass retention, it would require much higher simulation time. Nominal reactor volume was arbitrarily chosen equal to 4.4 L and headspace volume equal to 1.6 L. Working temperature was in the mesophilic range (i.e. 35 °C). The composition of the simulated influent was based on the characterization of slaughterhouse wastewater with a COD concentration of 15 kgCOD/m^3 and operated for 750 days under constant loading rate of 1.75 kgCOD/m^3 day. This influent consisted

Table 1 – Input concentrations of the slaughterhouse wastewater used during the simulations of the toxicant present in the feeding line.

Component	Values (kg COD/m^3)	Component	Values (kg COD/m^3)
Total VFAs	1.08	Inorganic carbon	2.51 mM C
Carbohydrates	2.35	Inorganic nitrogen	8.91 mM N
Proteins	6.71	Total dissolved COD	1.54
Lipids	2.51	Total particulate COD	13.47

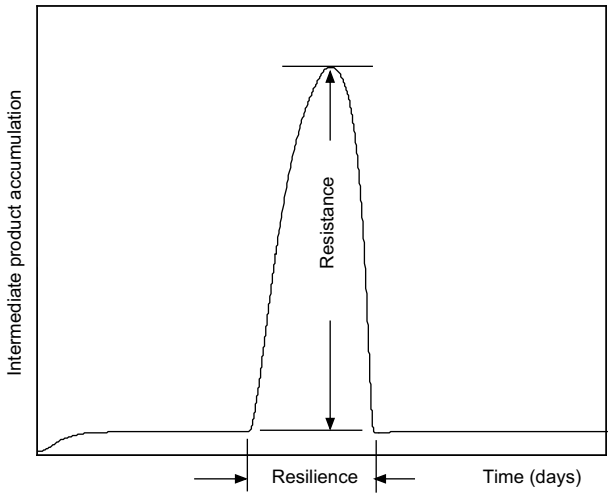

Fig. 3 – Definition of ecological parameters of functional stability. The amplification envelope is the overall plot.

mainly of carbohydrates, proteins, lipids, VFAs, inorganic carbon and inorganic nitrogen. The concentrations of these individual components used during simulations as process inputs are shown in Table 1.

The behavior of ADM1 and ADM1_10 has been compared in terms of biomass evolution and reactor performance before, during and after a temporarily increase in the influent TAN concentration (from 13 to 110 mM applied between day 150 and 200). The transition period and acclimatization were judged by traditional reactor performance indicators such as methane production rate (MPR), soluble COD removal and effluent volatile fatty acid (VFA) concentrations.

The diversity of the microbial community has been quantified by Simpson's reciprocal diversity index ($DI_{Simpson}$), calculated as follows:

$$DI_{Simpson}(t) = \frac{1}{\sum_{i=1}^{N} p_i(t)^2} \quad (1)$$

in which $p_i(t)$ represents the biomass fraction of species i in the considered (sub)population of *Bacteria* and *Archaea*, at a given time instant t. Microbial population concentrations lower than 10^{-3} kgCOD/m^3 were not considered in diversity indices calculations, to avoid accounting of species that are too diluted to be measured in practice.

It is clear that a higher Simpson diversity index corresponds with a more diverse population. The usefulness of this index to encode accurate information from microbial fingerprinting profiles has been demonstrated by He and Hu (2005).

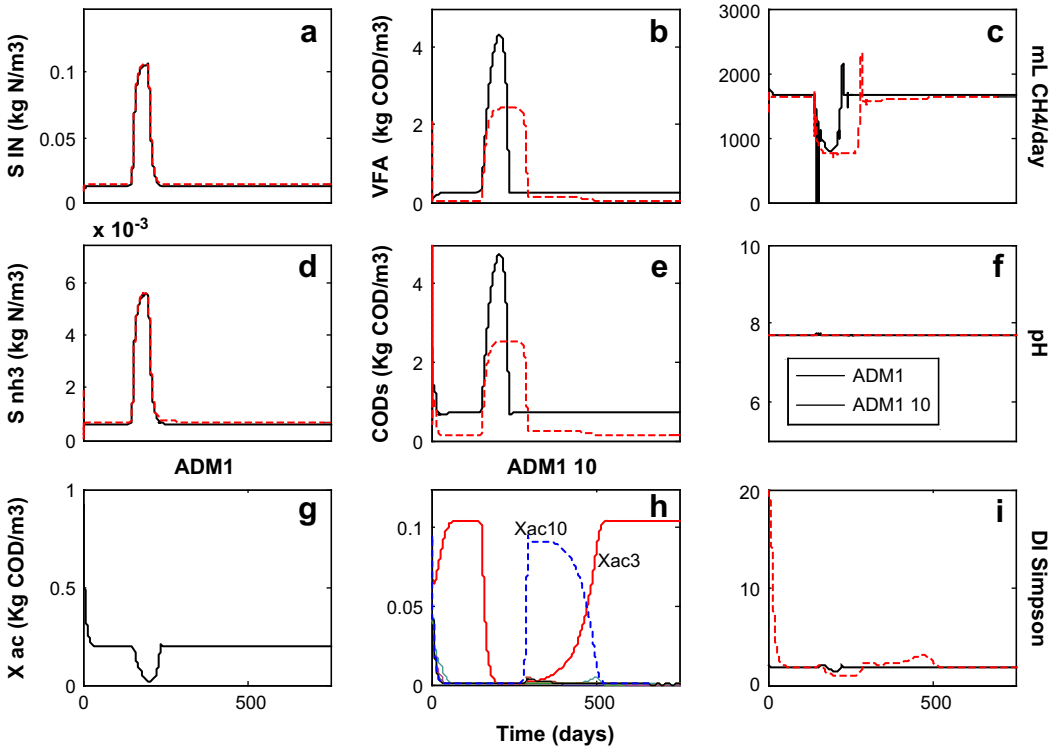

Fig. 4 – Comparison between ADM1 (full lines) and ADM1_10 (dotted line) for a reactor facing an ammonium pulse. Simulation results are presented in terms of total ammonium S_{IN} (a), VFA concentration (b), methane production rate (c), free ammonia (d), soluble COD (e), pH (f), evolution of acetate degraders (g, for ADM1, and h, for ADM1_10) and Simpson diversity index (i). Apart from the inhibition constant for ammonia, kinetic parameters were identical to those used in the simulations presented in Figs. 1 and 2.

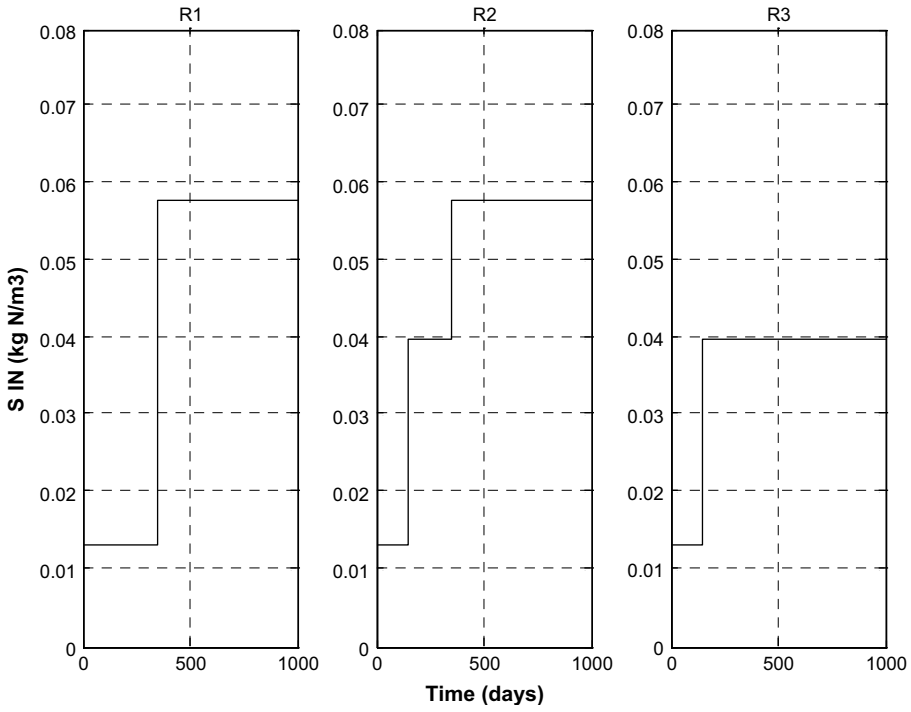

Fig. 5 – TAN concentration patterns for three feeding strategies (R1, R2 and R3) of increasing ammonia in the feeding line.

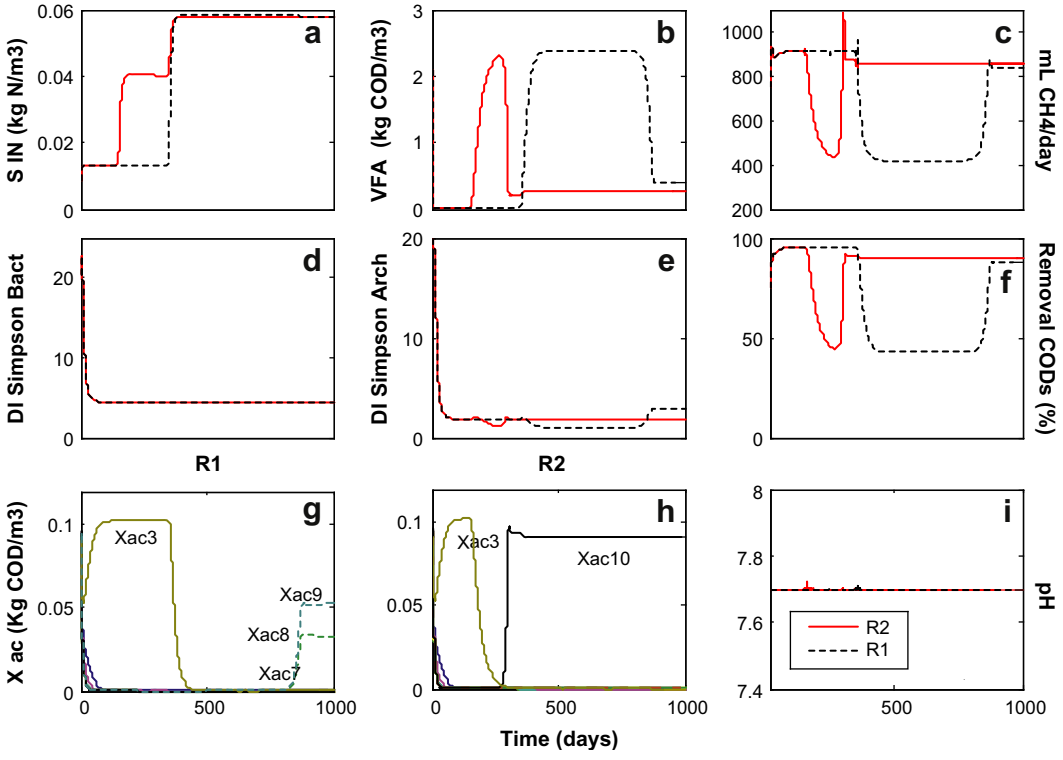

Fig. 6 – Simulated reactor performance with ADM1_10 for one-step (R1, from 13 to 58 mM, dotted line) and two-step (R2, from 13 to 40 mM and 40 to 58 mM, full line) ammonia increase in feeding line. Results are presented in terms of total ammonium S_{IN} (a), VFA concentration (b), methane production rate (c), Simpson diversity indices for Bacteria (d) and Archaea (e), soluble COD removal (f), evolution of acetate degraders (g, for R1, and h, for R2) and pH (i).

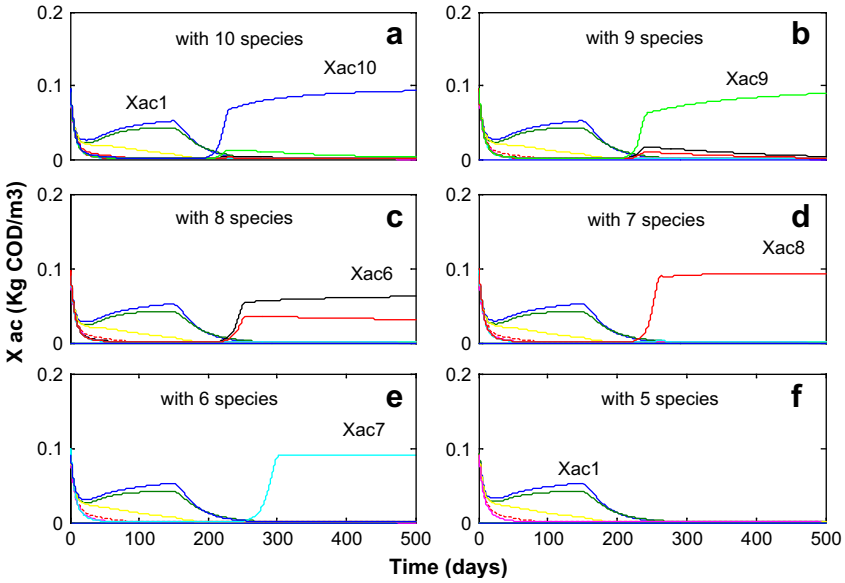

Fig. 7 – Simulated reactor performance with ADM1_10 for one-step ammonia increase in feeding line (R3, from 13 to 40 mM): selection of acetoclastic methanogens at successive suppression of the dominant species.

To investigate the effect of non-reactive toxicant such as ammonia that acts on specific populations, in this case methanogens, the inhibition constant for ammonia $K_{I,NH3}$ was modified. In line with the choice of the kinetic parameters of ADM1_10, the values of the inhibition constant for ammonia was randomly chosen from a normal bimodal distribution with means: $\mu_1 = 0.6 \times K_{I,NH3}$ (in this case it is assumed that some archaea species are much more sensitive to the presence of ammonia), $\mu_2 = 1.4 \times K_{I,NH3}$ (to represent the fact that some archaea species can be more tolerant) and standard deviations $\sigma_{1,2} = 0.125 \times K_{I,NH3}$.

To measure functional stability, we adopted parameters described in ecology (Grimm et al., 1992; Neubert and Caswell, 1997) in terms of the amplification envelope of key intermediate products in response to a perturbation (Fig. 3). The two main parameters obtained from this envelope are resistance and resilience. Resistance of a community with respect to an intermediate product is defined as the maximum accumulation of the product. It is a measure of the buffering capacity of the community with respect to the corresponding intermediate products (in our case, the different VFAs). Resilience is defined as the time taken by the accumulated intermediate product to return to its referential state (Neubert and Caswell, 1997). In this way, a higher numerical value denotes lower resistance or resilience. In general, the biodiversity is thought to be positively related to ecosystem stability in terms of resistance and resilience (Reinthaler et al., 2005; Saikaly et al., 2005).

Fig. 4 compares the simulated reactor response to the addition of toxicant (from day 150 to 200, see Fig. 4a and d) for ADM1 and ADM1_10.

The microbial community diversity from ADM1_10 is higher than for ADM1, as reflected through Simpson's diversity index (Fig. 4i) and displays more resistance (less accumulation of VFA and CODs, Fig. 4b and e). Nevertheless, the microbial community in ADM1_10 exhibits less resilience in response to TAN shocks (reflected by a larger recovery period). So, the biodiversity acts as insurance for CSTR functions against temporal changes in environmental factors like pulsed TAN, because removal soluble COD from ADM1 is lower than the ADM1_10 one during the perturbation period.

These simulation results agree with previous findings (Fernandez et al., 2000) where the responses of two continuously mixed methanogenic reactors, designated as high-spirochete (HS) and low-spirochete (LS) sets, were analyzed with respect to substrate (glucose)-loading shocks. The microbial community diversity of the latter (LS) was higher than the former one (HS), but displayed more resistance and less resilience, in response to glucose shocks.

Fig. 4g and h displays the evolution of acetate degraders for ADM1 and ADM1_10, respectively. For both models, the pulse increase of ammonia in the reactor results in a temporary decrease of the total amount of acetate degraders. The time to return to the total amount of acetate degraders present before the pulse is longer for ADM1_10 than for ADM1, again indicating the lower resilience of the former. Fig. 4h also reveals a population shift induced by the ammonia pulse: whereas species 3 is initially dominating, it is replaced with species 10, which is less inhibited by ammonium (higher $K_{I,NH3}$ value, see Table 2); once the ammonium concentration has decreased again, species 3 again wins the competition.

3.3. *Relationships between reactor performance and microbial community structure (facing increasing levels of ammonia with ADM1_10)*

In this section, ADM1_10 is applied to simulate the behavior of a CSTR for three different TAN concentration feeding strategies summarized in Fig. 5.

Table 2 – Biochemical parameters for the different acetate degraders.

Number of species	$\mu_{max,ac}$	$K_{S,ac}$	$K_{I,NH3}$	$Inhib_{ac}$	J^*_{ac}
1	0.2892	0.0197	0.0014	0.3937	0.2208
2	0.3281	0.0284	0.0012	0.3672	0.7854
3	0.3114	0.0477	0.0010	0.3246	0.2492
4	0.2856	0.0195	0.0011	0.3366	0.0844
5	0.2563	0.0467	0.0009	0.2925	0.1167
6	0.5635	0.2704	0.0023	0.5186	0.2021
7	0.4850	0.2775	0.0026	0.5510	0.2439
8	0.5391	0.2941	0.0027	0.5619	0.2066
9	0.5590	0.2884	0.0028	0.5695	0.1865
10	0.5714	0.2472	0.0025	0.5400	0.1683

3.3.1. *One-step increase vs. two-step increase in TAN (R1 vs. R2)*

The destabilizing effect of a step increase in TAN concentration on the reactor performance is shown in Fig. 6 in terms of total ammonia (Fig. 6a), on methane production rate (MPR, Fig. 6c), soluble COD removal (Fig. 6f), and VFA concentrations (Fig. 6b). Biomass adaptation to increased TAN concentration is indicated by the fact that when the TAN was changed from 40 to 58 mM in R2 the reactor performance is not as disturbed as in R1 when the TAN was changed from 13 to 58 mM. As a result the time required for complete adaptation (i.e. return to steady state as noted by effluent VFAs concentrations, removal soluble COD and MPR) was longer in R1 than in R2. These observations on slaughterhouse reactors are similar to those of van Velsen (1979), in studies of municipal sludge and piggery wastes in both adaptation time and disturbance grade. It is also clear from the simulation results that MPR and soluble COD removal efficiency decreased in the transition period (i.e. the time required for adaptation) and that these indices returned to lower levels than those obtained prior to the change in TAN concentration. Regarding the composition of the acetate degrading community (Fig. 6g and h), species 3 (i.e. *Xac3*) is dominant at the initial low TAN reactor concentrations, followed by a population shift for increasing TAN concentrations. The nature of this population shift depends on the different feeding strategies applied: R1 selects species 7 (i.e. *Xac7*), 8 (i.e. *Xac8*) and 9 (i.e. *Xac9*) (Fig. 6g), while R2 selects only the species 10 (i.e. *Xac10*) (Fig. 6h). This suggests that adaptation to elevated ammonia concentrations resulted from the selection of resistant acetoclastic methanogens (i.e. the species with high $K_{I,NH3}$) already present in seed sludge. The diversity indices plot indicates that the methanogenic activity was most affected (Fig. 6e), whereas the acetogenic and fermentative activities were not affected (Fig. 6d). These findings are in agreement with those of Calli et al. (2005), who, as already mentioned found a shift in archaea population during adaptation period under gradually increasing FAN levels.

3.3.2. *Effect of the suppression of species (R3)*

The selection of dominant acetoclastic methanogen species has subsequently been analyzed in more detail for a CSTR with a step increase in the TAN concentration from 13 to 40 mM at day 150 (Fig. 5, R3).

Fig. 7a shows the evolution of the 10 groups of acetate degraders initially present. Subsequently, the simulations have been rerun for a gradually restricted group of acetate

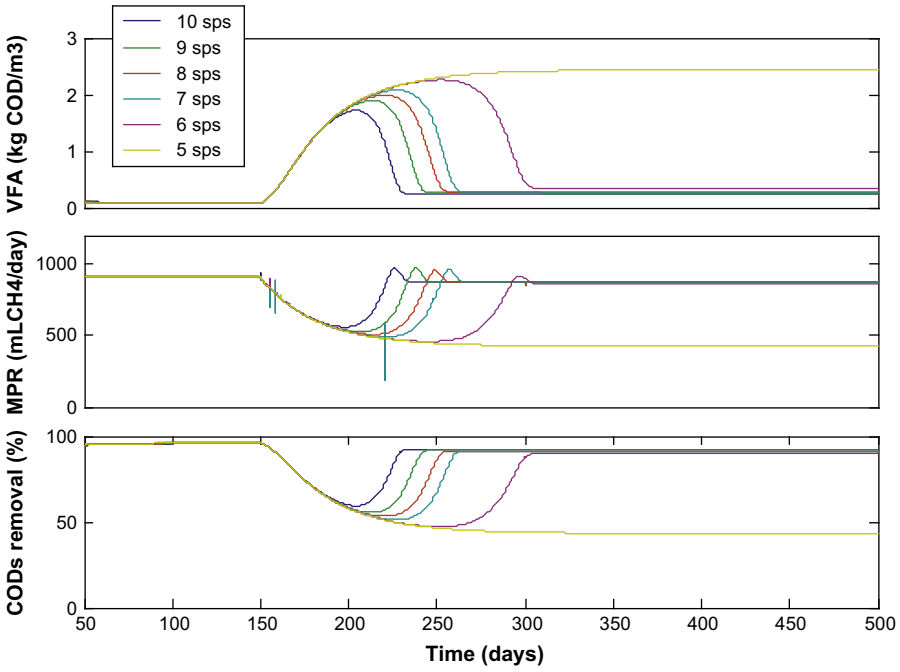

Fig. 8 – Macroscopic reactor performance corresponding with one-step ammonia increase in feeding line (R3, from 13 to 40 mM): VFA concentration, methane production rate and soluble COD removal for the simulations with successive suppression of the dominant species (see Fig. 7).

degraders, successively eliminating the winning species from the previous simulation. The results presented in Fig. 7b–f reveal the following ranking in order of decreasing competitive power: 10–9–6–8–7. Table 2 shows the values of the affinity constants and the maximum growth rates, which differ between the species. A common feature of all surviving species is their relatively high tolerance towards ammonium (high $K_{I,NH3}$); the reactor did not recover when only the more sensitive species (1–5) are present (Fig. 7f). Regarding the order of species selection, one may expect that species with a high substrate affinity (low K_S) or a high maximum growth rate (μ_{max}) have a competitive advantage. However, the ranking cannot be explained only in terms of either decreasing K_S or increasing μ_{max}, which would yield an order 10–6–9 rather than 10–9–6. As we explained below, the inhibition constant for ammonia ($K_{I,NH3}$) also plays a role.

A theoretical basis to understand species selection is given by Hsu et al. (1977), who have defined criteria for the outcome of microbial competition for a single limiting substrate in a CSTR operated under constant with a constant dilution rate and for a constant influent substrate concentration. They have defined:

$$J_{ac}(i) = K_{S,ac}(i)\frac{D}{\mu_{max,ac}(i) - D} \quad (2)$$

in which D represents the dilution rate.

If the number of competing species is such that their J_{ac}'s are ordered, with:

$$J_{ac}(1) < J_{ac}(2) < \cdots < J_{ac}(10)$$

all species die out if $S_{ac}(0) < J_{ac}(1)$. On the other hand, if $S_{ac}(0) > J_{ac}(i)\ \forall i$, then only species 1 (i.e. the one associated to $J_{ac}(1)$) survives and outcompetes all rival species. This principle has been verified experimentally by Hansen and Hubbell (1980).

An analogous J_{ac}-expression has been defined for our case where inhibition is present as follows:

$$J_{ac}(i)* = K_{S,ac}(i)\frac{D}{\mu_{max,ac}(i) * \mathrm{Inhib}_{ac}(i) - D}$$

The maximum growth rate has been corrected for inhibition effects through the same inhibition factor that we used for uptake of acetate in both models, i.e. $\mathrm{Inhib}_{ac} = I_{pH} \times I_{IN} \times I_{nh3}$ (see Appendix A). Note that the mathematical rigorousness of the criterion of Hsu et al. (1977), valid for a single substrate, expires in our case, since NH_3 acts as an additional substrate during acetate degradation (even though not limiting). Moreover, the acetate degradation reaction is only one step in the anaerobic digestion reaction network, while Hsu's criterion (see Eq. (2)) holds for single reaction systems. Despite these uncertainties, the obtained species ranking 10–9–6–8–7 in terms of increasing J^*_{ac} values agrees with the simulation results. The results indicate the advantage of criteria to predict the outcome of interspecies competition and may stimulate further research in this direction for models involving multiple reactions in series and/or parallel and including inhibition.

Fig. 8 displays the macroscopic reactor performance corresponding to Fig. 7 when the dominant species were successively suppressed. Note that the total initial biomass concentrations are the same in all simulations. The steady state behavior before and after the step was slightly influenced by the properties of the underlying microbial species. Nevertheless, the dynamic behavior in terms of the length of the acclimatization was significantly influenced by the microbial properties. The plot also reveals that the adaptation period gets lower when the number of resistant species at high TAN concentration levels (richness) increases. When all resistant species (6th sps–10th sps) were suppressed, the performance of the reactor did not recover. The process is running stably but with VFAs accumulation, lower MPR and higher effluent soluble COD, a condition termed ''inhibited steady state'' (Angelidaki and Ahring, 1993).

This example clearly illustrates that, although a different microbial composition may sometimes not seem to influence the macroscopic reactor behavior (the steady state conditions before and after the influent ammonia step increase are the same), another moment they may induce significantly different effects (response to increased toxic loads). This strengthens our belief that the engineering of wastewater treatment systems would be improved if one could predict and manipulate the associated microbial diversity. This ability would complement our established capacity to predict the optimal process design. Mathematical models, in which data on micro-scale molecular diversity, as gained with modern molecular tools (such as denaturant gradient gel electrophoresis – DGGE – fluorescent in situ hybridization with DNA probes – FISH. If this late is combined with a confocal laser-scanning microscope will allow the visualization of three-dimensional microbe structures, Sanz and Kochling, 2007), have been incorporated to more closely represent wastewater treatment processes, can provide a useful tool to reach this goal.

A credible model to predict the nature, composition and distribution of the microbial community can indeed allow us to explain how microbial diversity could vary with environmental conditions. Since the type of microorganisms present in a reactor ultimately defines its operational performance, this information can be of the utmost importance. Even though we do not yet know exactly the diversity of the different functional groups or how this diversity is sustained, the approach applied in this paper can be used to gain insight in the influence of process conditions on the selection of certain types of species and in our general belief, handle microbial diversity. In a later stage, this model can also be used to develop efficient control strategies adapted to model-based population optimization, but further work is clearly needed before engineers could use it to design a system.

4. Conclusions and perspectives

A methodology to account for microbial diversity in complex but structured models such as the anaerobic digestion model ADM1 has been presented. This approach consists of extending the number of mass balances for an arbitrary

number of species having the same function (performing the same reaction), while using a stochastic mechanism to select the corresponding microbial parameters. The resulting model remains powerful in representing macroscopic experimental data, but is moreover able to get insight in underlying microscopy. This has been demonstrated by investigating the impact of increasing toxicant concentrations and assessing the relationship between biodiversity and reactor performance.

Adaptation of microorganisms to inhibitory substances, as suggested in this paper, can significantly improve wastewater treatment efficiency. For instance, adaptation to elevated ammonia concentrations may result from the selection of resistant acetoclastic methanogens already present in seed sludge. The influence of microbial parameters of resistant acetoclastic methanogen species at high ammonia levels affecting interspecies competition has been assessed explicitly.

To deal with microbial diversity, the number of species considered for each biological reaction is arbitrary and in this study was set to 10, which is sufficient to demonstrate the potential of modeling microbial diversity. Besides, the number of species considered may differ between different functional groups (reactions). Moreover, handling a very high number of species per reaction (e.g. 100–1000) can be seen as a way to reduce efforts required for parameter estimation. Indeed, only a ''global'' value of the model parameters such as in ADM1 would be required, microbial diversity being later accounted for by the high number of species handled with random kinetic parameters centered around the average values found to fit ADM1.

Application of the presented methodology to represent – but not predict or engineer – biodiversity in other structured models, such as activated sludge models (ASMs) is straightforward. This offers wide perspectives not only in terms of modeling but also in terms of control objectives since microbial population appears nowadays to be a major component that drives process performances.

Acknowledgements

Ivan Ramirez thanks Veolia Environment R&D for their financial support. Dr. Eveline Volcke has been supported through a EU Marie Curie Intra-European Fellowship (EIF), Proposal 039401-PopCon4Biofilms, followed by a post-doctoral grant of the Flemish Fund for Scientific Research Foundation – Flanders (FWO). The authors also express their gratitude to Dr. Ulf Jeppsson and Dr. Christian Rosen, Lund University, Sweden, for providing the Matlab implementation of ADM1.

Appendix A.

Process kinetics and stoichiometry for sugar uptake and decay of sugar degraders in ADM1_10.

	ESTATES	1	2	3	4	5	6	7	8	9	10	11	12	13	14	15	16
	Component *i*	1	2	3	4	5	6	7	8	9	10	11	12	13	14	15	16
		Ssu	Saa	Sfa	Sva	Sbu	Spro	Sac	Sh2	Sch4	S_IC	S_IN	S_I	X_xc	X_ch	X_pr	X_li
j	Process																
1	Disintegration										*	**	f_SI_Xc	−1	f_ch_Xc	f_pr_Xc	f_li_Xc
2	Hydrolysis carbohydrates	1									*				1		
3	Hydrolysis proteins		1								*					1	
4	Hydrolysis lipids	1 − f_fa_li		f_fa_li							*						1
5(1)	Uptake of sugars by Xsu(1)	−1				(1 − Y_su(1))f_bu_su	(1 − Y_su(1))f_pro_su	(1 − Y_su(1))f_ac_su	(1 − Y_su(1))f_h2_su		*	(−Y_su(1)) × N_bac					
5(2)	Uptake of sugars by Xsu(2)	−1				(1 − Y_su(2))f_bu_su	(1 − Y_su(2))f_pro_su	(1 − Y_su(2))f_ac_su	(1 − Y_su(2))f_h2_su		*	(−Y_su(2)) × N_bac					
5(3)	Uptake of sugars by Xsu(3)	−1				(1 − Y_su(3))f_bu_su	(1 − Y_su(3))f_pro_su	(1 − Y_su(3))f_ac_su	(1 − Y_su(3))f_h2_su		*	(−Y_su(3)) × N_bac					
5(4)	Uptake of sugars by Xsu(4)	−1				(1 − Y_su(4))f_bu_su	(1 − Y_su(4))f_pro_su	(1 − Y_su(4))f_ac_su	(1 − Y_su(4))f_h2_su		*	(−Y_su(4)) × N_bac					
5(5)	Uptake of sugars by Xsu(5)	−1				(1 − Y_su(5))f_bu_su	(1 − Y_su(5))f_pro_su	(1 − Y_su(5))f_ac_su	(1 − Y_su(5))f_h2_su		*	(−Y_su(5)) × N_bac					
5(6)	Uptake of sugars by Xsu(6)	−1				(1 − Y_su(6))f_bu_su	(1 − Y_su(6))f_pro_su	(1 − Y_su(6))f_ac_su	(1 − Y_su(6))f_h2_su		*	(−Y_su(6)) × N_bac					
5(7)	Uptake of sugars by Xsu(7)	−1				(1 − Y_su(7))f_bu_su	(1 − Y_su(7))f_pro_su	(1 − Y_su(7))f_ac_su	(1 − Y_su(7))f_h2_su		*	(−Y_su(7)) × N_bac					
5(8)	Uptake of sugars by Xsu(8)	−1				(1 − Y_su(8))f_bu_su	(1 − Y_su(8))f_pro_su	(1 − Y_su(8))f_ac_su	(1 − Y_su(8))f_h2_su		*	(−Y_su(8)) × N_bac					
5(9)	Uptake of sugars by Xsu(9)	−1				(1 − Y_su(9))f_bu_su	(1 − Y_su(9))f_pro_su	(1 − Y_su(9))f_ac_su	(1 − Y_su(9))f_h2_su		*	(−Y_su(9)) × N_bac					
5(10)	Uptake of sugars by Xsu(10)	−1				(1− Y_su(10)) f_bu_su	(1 − Y_su(10)) f_pro_su	(1 − Y_su(10)) f_ac_su	(1 − Y_su(10)) f_h2_su		*	(−Y_su(10)) × N_bac					
6	Uptake of amino acids		−1		(1 − Y_aa) f_va_aa	(1 − Y_aa)f_bu_aa	(1 − Y_aa)f_pro_aa	(1 − Y_aa)f_ac_aa	(1 − Y_aa)f_h2_aa		*	(−Y_fa) × N_bac					
7	Uptake of LCFA			−1				(1 − Y_fa) × 0.7	(1 − Y_fa) × 0.3		*	(−Y_c4) × N_bac					
8	Uptake of valerate				−1		(1 − Y_c4) × 0.54	(1 − Y_c4) × 0.31	(1 − Y_c4) × 0.15		*	(−Y_c4) × N_bac					
9	Uptake of butyrate					−1		(1 − Y_c4) × 0.8	(1 − Y_c4) × 0.2		*	(−Y_pro) × N_bac					
10	Uptake of propionate						−1	(1 − Y_pro) × 0.57	(1 − Y_pro) × 0.43		*	(−Y_ac) × N_bac					
11	Uptake of acetate							−1		1 − Y_ac	*	(−Y_h2) × N_bac					
12	Uptake of hydrogen								−1	1 − Y_h2	*	N_bac-N_xc					
13(1)	Decay of Xsu(1)										*	N_bac-N_xc		1			
13(2)	Decay of Xsu(2)										*	N_bac-N_xc		1			
13(3)	Decay of Xsu(3)										*	N_bac-N_xc		1			
13(4)	Decay of Xsu(4)										*	N_bac-N_xc		1			
13(5)	Decay of Xsu(5)										*	N_bac-N_xc		1			
13(6)	Decay of Xsu(6)										*	N_bac-N_xc		1			
13(7)	Decay of Xsu(7)										*	N_bac-N_xc		1			
13(8)	Decay of Xsu(8)										*	N_bac-N_xc		1			
13(9)	Decay of Xsu(9)										*	N_bac-N_xc		1			
13(10)	Decay of Xsu(10)										*	N_bac-N_xc		1			
14	Decay of Xaa										*	N_bac-N_xc		1			
15	Decay of Xfa										*	N_bac-N_xc		1			
16	Decay of Xc4										*	N_bac-N_xc		1			
17	Decay of Xpro										*	N_bac-N_xc		1			
18	Decay of Xac										*	N_bac-N_xc		1			
19	Decay of Xh2										$*\sum_{i=1-9}^{11-87} C_i V_{i,j}$						

Appendix B.

Process kinetics and stoichiometry for sugar uptake and decay of sugar degraders in ADM1_10.

17(1)	17(2)	17(3)	17(4)	17(5)	17(6)	17(7)	17(8)	17(9)	17(10)	18 18 Xaa	19 19 Xfa	20 20 Xc4	21 21 Xpro	22 22 Xac	23 23 Xh2	24 24 X_I	Rate	
																f_XI_Xc	kr_dis × Xc	
																	k_hyd_ch × Xch	
																	k_hyd_pr × Xpr	
																	k_hyd_li × Xli	
Y_su(1)																	k_m_su(1) × Ssu/	
																	(K_S_su(1) + Ssu) × Xsu(1) × inhib[1]	
	Y_su(2)																k_m_su(2) × Ssu/	
																	(K_S_su(2) + Ssu) × Xsu(2) × inhib[1]	
		Y_su(3)															k_m_su(3) × Ssu/	
																	(K_S_su(3)+Ssu) × Xsu(3) × inhib[1]	
			Y_su(4)														k_m_su(4) × Ssu/	
																	(K_S_su(4) + Ssu) × Xsu(4) × inhib[1]	
				Y_su(5)													k_m_su(5) × Ssu/	
																	(K_S_su(6) + Ssu) × Xsu(5) × inhib[1]	
					Y_su(6)												k_m_su(6) × Ssu/	
																	(K_S_su(6) + Ssu) × Xsu(6) × inhib[1]	
						Y_su(7)											k_m_su(7) × Ssu/	
																	(K_S_su(7) + Ssu) × Xsu(7) × inhib[1]	
							Y_su(8)										k_m_su(8) × Ssu/	
																	(K_S_su(8) + Ssu) × Xsu(8) × inhib[1]	
								Y_su(9)									k_m_su(9) × Ssu/	
																	(K_S_su(9) + Ssu) × Xsu(9) × inhib[1]	
									Y_su(10)								k_m_su(10) × Ssu/	inhib[1] = I_pH_aa × I_IN_lim
																	(K_S_su(10) + Ssu) × Xsu(10) × inhib[1]	inhib[2] = inhib[1] × I_h2_fa
										Y_aa							k_m_aa × Saa/(K_S_aa + Saa) × Xaa × inhib[1]	inhib[3] = inhib[1] × I_h2_c4
											Y_fa						k_m_fa × S fa/(K_S_fa + Sfa) × Xfa × inhib[2]	inhib[4] = inhib[1] × I_h2_pro
												Y_c4					k_m_c4 × Sva/(K_S_c4 + Sva) × Xc4 × Sva/	inhib[5] = I_pH_ac × I_IN_lim × I_nh3
																	(Sva + Sbu + eps) × inhib[3]	
												Y_c4					k_m_c4 × Sbu/(K_S_c4 + Sbu) × Xc4 × Sbu/	inhib[6] = I_pH_h2 × I_IN_lim
																	(Sbu + Sva + eps) × inhib[3]	
													Y_pro				k_m_pro* Spro/(K_S_pro+Spro) × Xpro × inhib[4]	
														Yac			k_m_ac × S ac/(K_S_ac+Sac) × Xac × inhib[5]	I_IN_lim = 1/(1 + K_S_IN/SIN)
															Y_h2		k_m_h2 × Sh2/(K_S_h2 + Sh2) × Xh2 × inhib[6]	I_h2_c4 = 1/(1 + Sh2/K_Ih2_c4)
																		I_h2_c4 = 1/(1 + Sh2/K_Ih2_c4)
	−1																k_dec_Xsu(1) × Xsu(1)	I_h2_pro = 1/(1 + Sh2/K_Ih2_pro)
		−1															k_dec_Xsu(2) × Xsu(2)	
			−1														k_dec_Xsu(3) × Xsu(3)	
				−1													k_dec_Xsu(4) × Xsu(4)	
					−1												k_dec_Xsu(5) × Xsu(5)	
						−1											k_dec_Xsu(6) × Xsu(6)	
							−1										k_dec_Xsu(7) × Xsu(7)	
								−1									k_dec_Xsu(8) × Xsu(8)	
									−1								k_dec_Xsu(9) × Xsu(9)	
										−1							k_dec_Xsu(10) × Xsu(10)	
											−1						k_dec_Xaa × Xaa	I_nh3 = 1/(1 + xtemp[33]/K_I_nh3)
												−1					k_dec_Xfa × Xfa	
													−1				k_dec_Xc4 × Xc4	**(Nr_xc-f_xI_xc × N_I-f_sI_xc × N_I-f_pr_xc × N_aa)
														−1			k_dec_Xpro × Xpro	***(Ns_xc-f_xI_xc × N_I-f_sI_xc × N_I-f_pr_xc × N_aa)
															−1		k_dec_Xac × Xac	
																−1	k_dec_Xh2 × Xh2	

REFERENCES

Angelidaki, I., Ahring, B.K., 1993. Thermophilic anaerobic digestion of livestock waste: effect of ammonia. Appl. Microbiol. Biotechnol. 38, 560–564.

Batstone, D.J., Keller, J., Angelidaki, I., Kalyuzhnyi, S.V., Pavlostathis, S.G., Rozzi, A., Sanders, W.T.M., Siegrist, H., Vavilin, V.A., 2002. Anaerobic Digestion Model No. 1 (ADM1). IWA Scientific and Technical Report No. 13. IWA Publishing, London.

Borja, R., Sanchez, E., Weiland, P., 1996. Influence of ammonia concentration on thermophilic anaerobic digestion of cattle manure in upflow anaerobic sludge blanket (UASB) reactors. Process Biochem. 31 (5), 477–483.

Calli, B., Mertoglu, B., Inanc, B., Yenigun, O., 2005. Community changes during start-up in methanogenic bioreactors exposed to increasing levels of ammonia. Environ. Technol. 26, 85–91.

Chen, Y., Cheng, J., Creamer Kurt, S., 2008. Inhibition of anaerobic digestion process: a review. Bioresour. Technol. 99 (10), 4044–4064.

Fernandez, A.S., Hasham, S.A., Dollhope, S.L., Raskin, L., Glagoleva, O., Dazzo, F.B., Hickey, R.F., Criddle, C.S., Tiejed, J. M., 2000. Flexible community structure correlates with stable community function in methanogenic biorector communities perturbed by glucose. Appl. Environ. Microbiol. 66 (9), 4058–4067.

Grimm, V., Schmidt, E., Wissel, C., 1992. On the application of stability concepts in ecology. Ecol. Model. 63, 143–161.

Hansen, K.H., Angelidaki, I., Ahring, B.K., 1998. Anaerobic digestion of swine manure: inhibition by ammonia. Water Res. 32, 5–12.

Hansen, S.R., Hubbell, S.P., 1980. Single-nutrient microbial competition: qualitative agreement between experimental and theoretically forecast outcomes. Science 207 (28), 1491–1493.

He, F., Hu, X.-S., 2005. Hubbell's fundamental biodiversity parameter and Simpson diversity index. Ecology Letters 8, 386–390.

Hsu, S.B., Hubbell, S., Waltman, P., 1977. A mathematical theory for single-nutrient competition in continuous cultures of micro-organisms. SIAM J. Appl. Math. 32 (2), 366–383.

Kotsyurbenko, O.R., 2005. Trophic interactions in the methanogenic microbial community of low-temperature terrestrial ecosystems. FEMS Microbiol Ecol. 53 (1), 3–13.

Neubert, M.G., Caswell, H., 1997. Alternatives to resilience for measuring the responses of ecological systems to perturbation. Ecology 78, 653–665.

Rajinikanth, R., Ramirez, I., Steyer, J.P., Mehrotra, I., Kumar, P., Escudie, R., Torrijos, M., 2008. Experimental and modeling investigations of a hybrid upflow anaerobic sludge-filter bed (UASFB) reactor. Water Sci. Technol. 58 (1), 109–117.

Ramirez, I., Steyer, J.P., 2008. Modeling microbial diversity in anaerobic digestion. Water Sci. Technol. 57 (2), 265–270.

Reinthaler, T., Winter, C., Herndl, G.J., 2005. Relationship between bacterioplankton richness, respiration, production in the southern North Sea. Appl. Environ. Microbiol. 71 (5), 2260–2266.

Saikaly, P.E., Stroot, P.G., Oerther, D.B., 2005. Use of 16S rRNA gene terminal restriction fragment analysis to assess the impact of solids retention time on the bacterial diversity of activated sludge. Appl. Environ. Microbiol. 71 (10), 5814–5822.

Sanz, J., Kochling, T., 2007. Molecular biology techniques used in wastewater treatment: an overview. Process Biochem. 42, 119–133.

Sprott, G.D., Patel, G.B., 1986. Ammonia toxicity in pure cultures of methanogenic bacteria. Syst. Appl. Microbiol. 7, 358–363.

Tilman, D., Knops, J., Wedin, D., Reich, P., 2002. Experimental and observational studies of diversity, productivity, and stability. In Kinzig, A., Pacala, S., Tilman, D. (Eds.), Functional Consequences of Biodiversity: Empirical Progress and Theoretical Extensions. Princeton University Press, Princeton, NJ, USA, pp. 42–70.

van Velsen, A.F.M., 1979. Adaptation of methanogenic sludge to high ammonia-nitrogen concentration. Water Res. 13, 995–1001.

Volcke, E.I.P., Sanchez, O., Steyer, J.P., Dabert, P., Bernet, N., 2008. Microbial population dynamics in nitrifying biofilm reactors: experimental evidence described by a simple model including interspecies competition. Process Biochem. 43, 1398–1406.

Wiegant, W., Zeeman, G., 1986. The mechanism of ammonia inhibition in the thermophilic digestion of livestock wastes. Agric. Wastes 16, 248–253.

Yuan, Z., Blackall, L., 2002. Sludge population optimisation, a new dimension for the control of biological wastewater treatment systems. Water Res. 36 (2), 482–490.